

Original research article

Esrrb function is required for proper primordial germ cell development in presomite stage mouse embryos

Eiichi Okamura^{a,b,*}, Oliver H. Tam^{a,1}, Eszter Posfai^{a,2}, Lingyu Li^{a,3}, Katie Cockburn^{a,4}, Cheryl Q.E. Lee^{a,5}, Jodi Garner^{a,6}, Janet Rossant^{a,c,**}

^a Program in Developmental and Stem Cell Biology, Hospital for Sick Children, Toronto, Ontario, Canada

^b Graduate School of Biomedical Sciences, Tokushima University, Tokushima, Japan

^c Department of Molecular Genetics, University of Toronto, Toronto, Ontario, Canada

A B S T R A C T

Estrogen related receptor beta (Esrrb) is an orphan nuclear receptor that is required for self-renewal and pluripotency in mouse embryonic stem (ES) cells. However, in the early post-implantation mouse embryo, *Esrrb* is specifically expressed in the extraembryonic ectoderm (ExE) and plays a crucial role in trophoblast development. Previous studies showed that *Esrrb* is also required to maintain trophoblast stem (TS) cells, the *in vitro* stem cell model of the early trophoblast lineage. In order to identify regulatory targets of *Esrrb* *in vivo*, we performed microarray analysis of *Esrrb*-null versus wild-type post-implantation ExE, and identified 30 genes down-regulated in *Esrrb*-mutants. Among them is *Bmp4*, which is produced by the ExE and known to be critical for primordial germ cell (PGC) specification *in vivo*. We further identified an enhancer region bound by *Esrrb* at the *Bmp4* locus by performing *Esrrb* ChIP-seq and luciferase reporter assay using TS cells. Finally, we established a knockout mouse line in which the enhancer region was deleted using CRISPR/Cas9 technology. Both *Esrrb*-null embryos and enhancer knockout embryos expressed lower levels of *Bmp4* in the ExE, and had reduced numbers of PGCs. These results suggested that *Esrrb* functions as an upstream factor of *Bmp4* in the ExE, regulating proper PGC development in mice.

1. Introduction

Germ cells are the only cell types capable of creating life for the next generation in animals employing sexual reproduction. There are at least two distinct mechanisms for the specification of the germ cell lineage in multi-cellular organisms (Extavour and Akam, 2003). One is known as preformation wherein primordial germ cells (PGCs) are determined by preformed germ plasm inherited from the egg. This mode is seen in many model organisms including *Caenorhabditis elegans*, *Drosophila melanogaster*, *Danio rerio*, and *Xenopus laevis*. The other mode that is seen in mammals is known as germ cell induction. In this mode, germ cells cannot be identified until later in development and PGCs are induced by signals from surrounding somatic tissues. The mechanisms of PGC induction are well studied in mice, in which signals from the ExE and visceral endoderm (VE) play an essential role in the induction of PGCs

around embryonic day (E) 6.5 (de Sousa Lopes et al., 2007; de Sousa Lopes et al., 2004; Yoshimizu et al., 2001). Among them, *Bmp4* signaling from the ExE is primarily required for epiblast (EPI) cells to gain germ-line competency (Lawson et al., 1999; Pesce et al., 2002). The synergistic action of *Bmp4* and *Bmp8b*, which are both secreted by the ExE, induce PGC precursors in a dose-dependent manner in the underlying EPI (Ying et al., 2001). In addition, *Bmp2* from the proximal VE enhances the same signaling pathway along with *Bmp4* and ensures that the highest levels of BMP signaling occurs in the most proximal EPI (Ying and Zhao, 2001). Consistently, targeted disruption of BMP signaling components, including *Bmp2*, *Bmp4*, *Bmp8b*, *Smad1*, *Smad4*, *Smad5* and *Alk2*, cause reduction of PGC numbers in embryos (Chang and Matzuk, 2001; Chu et al., 2004; de Sousa Lopes et al., 2004; Hayashi et al., 2002; Lawson et al., 1999; Tremblay et al., 2001b; Ying et al., 2000; Ying and Zhao, 2001). Thus, a requirement of BMP signaling for PGC specification

* Corresponding author. Graduate School of Biomedical Sciences, Tokushima University, Tokushima, Japan.

** Corresponding author. Program in Developmental and Stem Cell Biology, Hospital for Sick Children, Toronto, Ontario, Canada.

E-mail addresses: okamura.eiichi@tokushima-u.ac.jp (E. Okamura), janet.rossant@sickkids.ca (J. Rossant).

¹ Cold Spring Harbor Laboratory, Cold Spring Harbor, New York, USA.

² Department of Molecular Biology, Princeton University, New Jersey, USA.

³ Refuge Biotechnologies Inc, Menlo Park, CA, USA.

⁴ Dept. of Genetics, Yale School of Medicine, New Haven, CT, USA.

⁵ Institute of Medical Biology, Singapore.

⁶ Ontario Institute for Regenerative Medicine, Toronto, Ontario, Canada.

<https://doi.org/10.1016/j.ydbio.2019.07.008>

Received 18 February 2019; Received in revised form 12 July 2019; Accepted 12 July 2019

Available online 14 July 2019

0012-1606/© 2019 Elsevier Inc. All rights reserved.

in mice is well established.

However, the regulatory mechanism leading to *Bmp4* expression in extraembryonic regions remains unknown. Stem cell lines have been widely used to study early mammalian development, as the limited number of cells obtained from early embryos is often insufficient to conduct biochemical or molecular biological experiments. From the trophoblast (TE) of the preimplantation embryo or from the ExE, an early post-implantation descendant of the TE, trophoblast stem (TS) cells can be derived (Tanaka et al., 1998). TS cells retain the nature of cells in ExE and can differentiate into multiple cell types of the trophoblast lineage. In the past, several transcription factors required for maintaining the stem cell state of TS cells have been identified, including *Cdx2*, *Eomes*, *Elf5*, *Sox2*, *Tfap2c* and *Esrrb* (Adachi et al., 2013; Donnison et al., 2005; Kidder and Palmer, 2010; Strumpf et al., 2005; Tremblay et al., 2001a). Among them, an orphan nuclear receptor *Esrrb* (estrogen related receptor beta) was reported to sustain stemness by directly binding and regulating TS cell-specific genes under the control of the FGF signaling pathway (Latos et al., 2015). Interestingly, the direct target genes of *Esrrb* identified by transcriptome and chromatin immunoprecipitation (ChIP)-sequencing (seq) analysis in the aforementioned study included *Bmp4*. This suggested that *Esrrb* might function as an upstream regulatory factor of *Bmp4* in the ExE, and thereby enhance PGC specification *in vivo*.

To test this hypothesis *in vivo*, we investigated the gene expression profile of the ExE in *Esrrb*-null embryos and showed that *Bmp4* is among those genes whose expression is significantly decreased compared to wild-type controls. By then employing TS cells, we characterized an enhancer region bound by *Esrrb* at the *Bmp4* locus. *Esrrb*-null and enhancer knockout embryos showed reduced numbers of PGCs, demonstrating that *Esrrb* directly regulates *Bmp4* transcription in the ExE and is required for proper PGC specification in mice.

2. Results and discussion

2.1. *Esrrb* deficiency results in altered transcriptional profiles in the early ExE

Esrrb is expressed in the oocyte and throughout cleavage stage embryos in the mouse (Goolam et al., 2016), and is later restricted to the inner cell mass (ICM) at the blastocyst stage (Adachi et al., 2013; Guo et al., 2010). However, expression is known to switch to the trophoblast lineage from the EPI lineage by early post-implantation stage (Festuccia et al., 2018; Luo et al., 1997). To examine the dynamic expression pattern of *Esrrb* in detail, we performed immunofluorescence analysis in peri-implantation mouse embryos. *Esrrb* was expressed only in the ICM in E4.5 blastocyst embryos cultured *in vitro* (Fig. 1A). However, in E4.75 embryos flushed from the uterus, which were likely to have been implanting, *Esrrb* was expressed not only in ICM but also in the polar TE overlying the ICM that would later give rise to ExE (Fig. 1B). In the early post-implantation E5.5 mouse conceptus, *Esrrb* could be detected only in the ExE, where it will become progressively confined to the chorionic ectoderm rather than the ectoplacental cone (Fig. 1C). We also detected non-nuclear fluorescent signal in the visceral endoderm (VE) region, which we believe is from non-specific binding of the antibody, an observation that has been previously reported by another group (Adachi et al., 2013). The trophoblast lineage-restricted expression of *Esrrb* persists to E6.5, where we observed only ExE-specific transcription by *in situ* hybridization analysis (Fig. 1D). Thus, we clearly showed that *Esrrb* is activated in the trophoblast lineage from E4.75 and disappears from the EPI lineage between E4.75 to E5.5. By E8.5, when the chorion fuses with the ectoplacental cone, *Esrrb* expression starts to decline and is eventually extinguished (Luo et al., 1997; Pettersson et al., 1996).

It has been previously reported that homozygous *Esrrb* mutant mice do not exhibit gross morphological defects in the extra-embryonic region at E6.5, with mutant phenotypes, such as the absence or hypoplasia of the chorion, manifesting only by E7.5 (Luo et al., 1997). To examine if *Esrrb*

already exerts a regulatory effect on gene expression in the trophoblast lineage at E6.5, around which time PGC precursors are being induced, we dissected the ExE regions from wild-type and mutant embryos (Fig. 1D). Dissected ExE tissues with overlying VE from 20 to 25 embryos were pooled based on genotype, and differential gene expression was assessed by microarray with three replicates for both wild-type and *Esrrb* mutant samples. We uncovered 27 genes that were significantly ($FDR < 0.05$) up-regulated and 30 genes (including *Bmp4*, *Elf5* and *Sox2*) that were down-regulated in the absence of *Esrrb* (Fig. 1E and F). A subset of them was confirmed by RT-qPCR analysis (Supplemental Figs. S1 and S2). Additionally, we demonstrated that *Bmp4* and *Sox2* expression were significantly decreased in the *Esrrb* mutant ExE, using *in-situ* hybridization (Fig. 1D).

2.2. *Esrrb* directly regulates *Bmp4* transcription in TS cells

Latos et al. reported direct target genes of *Esrrb* in TS cells, including *Bmp4* (Latos et al., 2015). To confirm this result, we first treated TS cells with a synthetic *Esrrb* inhibitor Diethylstilbestrol (DES) or vehicle (Supplemental Fig. S3) and compared their global gene expression profile via RNA-seq analysis. We identified 1879 and 2053 genes significantly ($FDR < 0.05$) down- and up-regulated by DES treatment, respectively (Fig. 2A and B, Supplemental Table S1). We confirmed down-regulation of *Bmp4*, *Elf5* and *Sox2* expression by RT-qPCR (Fig. 2C). Consistent with DES treatment, knockdown of *Esrrb* in TS cells by two independent shRNA expression vectors also resulted in a tendency towards down-regulation of *Bmp4*, *Elf5* and *Sox2* (Supplemental Fig. S4). *Esrrb* inhibition or knockdown causes TS cells to differentiate, therefore in principle, it is possible that these transcriptional changes were due to differentiation. In our study, the change in *Cdx2* expression, a stemness marker of TS cells, was minimal after 48 h following *Esrrb* inhibition or after 72 h following knockdown vector transfection, and only longer DES exposure or more efficient *Esrrb* knockdown caused significant reduction of *Cdx2* expression, as observed in the previous study (Latos et al., 2015). Thus we hypothesized that *Esrrb* may function as a direct upstream regulator of these genes in TS cells.

To test this, we performed *Esrrb* ChIP-seq in TS cells. Motif enrichment analysis of ChIP peaks revealed that *Esrrb* mainly binds to the canonical *Esrrb* binding motif (BAAGGTCA) in TS cells (Supplemental Table S2). We integrated the *Esrrb* ChIP-seq data with the RNA-seq results using the software package Binding and Expression Target Analysis (BETA) (Wang et al., 2013). This algorithm predicts direct target genes by combining the binding potential from ChIP-seq data with differential expression data. Because it uses a distance-weighted measure to gauge the regulatory potential of all the binding sites of the factor within a certain distance (our setting: 100 kb), genes with more proximal binding and more differential expression are more likely to be called as real targets. We identified 622 genes (320 up regulated and 302 down regulated genes upon *Esrrb* inhibition) as potential transcriptional targets of *Esrrb* in TS cells (Supplemental Tables S3 and S4), of which 8 genes (*Bmp4*, *Apcdd1*, *NrOb1*, *C77370*, *Elf5*, *Adams3*, *Marcks* and *Gcnt4*) were also differentially expressed between wild-type and *Esrrb* knockout embryos (Fig. 2A and B). Thus, our data suggested that *Bmp4* (among others) is a direct target of *Esrrb*-mediated transcriptional regulation in TS cells.

2.3. Enhancers associated with *Bmp4* are regulated by *Esrrb* in TS cells

A previous study by Murohashi and colleagues identified a 1.4 kb putative trophoblast enhancer element in the 5'-flanking region of the *Bmp4* gene, termed “*Bmp4*-5' -1.4 kb” (Murohashi et al., 2010) (Fig. 3A and B). They narrowed down enhancer activity with a luciferase reporter assay in TS cells to two crucial regions within “*Bmp4*-5' -1.4 kb”: one located at -2118 to -1928 bp and the other at -1516 to -949 bp from the *Bmp4* transcription start site. They reported that *Cdx2* is one of the factors that binds to the -2118 to -1928 region, but transcription factor binding to the -1516 to -949 region had not been identified yet.

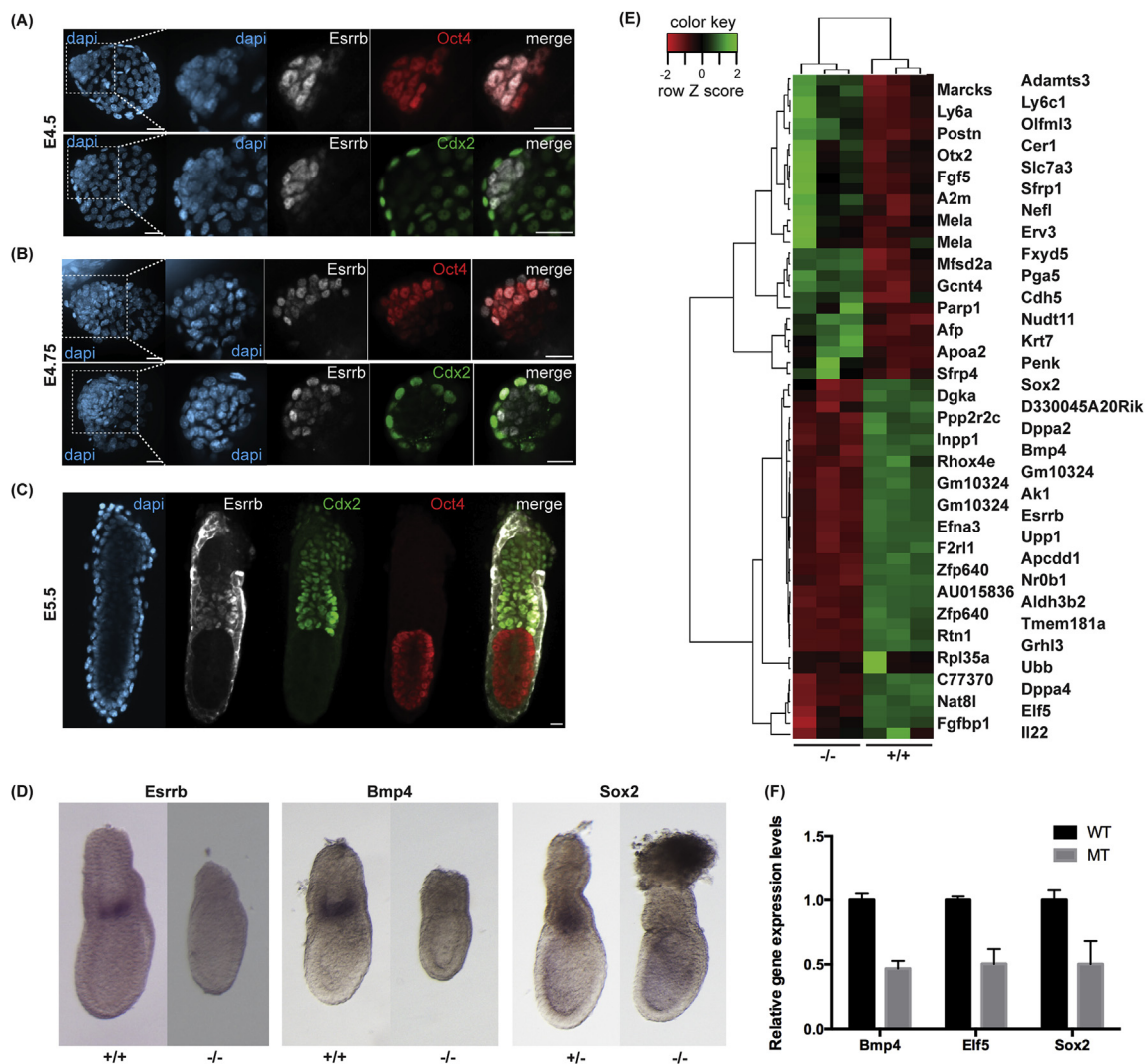


Fig. 1. Differences in gene expression between wild-type and *Esrrb* knockout mouse embryos. (A, B and C) Immunofluorescence distribution of *Esrrb* (white), together with lineage-specific markers for trophoblast (*Cdx2*, green) and pluripotent epiblast (*Oct4*, red) in wild-type E4.5 (A) and E4.75 (B) pre-implantation embryos and E5.5 (C) post-implantation embryos. 13 E4.5, 9 E4.75 and 13 E5.5 embryos were analyzed. Representative images are shown in the figure. Scale bar, 20 μ m. (D) *In situ* hybridization analysis of *Esrrb*, *Bmp4* and *Sox2* expression in wild-type and *Esrrb* knockout embryos. 4 wild-type (+/+) and 3 homozygous *Esrrb* knockout (-/-) E6.5 embryos were used for *Esrrb* analysis. 1 wild-type (+/+) and 2 homozygous *Esrrb* knockout (-/-) E6 embryos were used for *Bmp4* analysis. 2 heterozygous *Esrrb* knockout (+/-) and 1 homozygous *Esrrb* knockout (-/-) E6 embryos were used for *Sox2* analysis. Representative images are shown. (E) Heatmap of differentially expressed genes between wild-type (+/+) and homozygous *Esrrb* knockout (-/-) E6.5 ExEs in microarray analysis. 20–25 ExEs were pooled based on genotype, and three replicates for both wild-type and *Esrrb* homozygous knockout samples were prepared. (F) Comparison of relative gene expression levels of *Bmp4*, *Elf5* and *Sox2* between wild-type (+/+) and homozygous *Esrrb* knockout (-/-) E6.5 embryos determined by microarray analysis.

Interestingly, our ChIP-seq results identified a genomic region within the -1516 to -949 fragment that was enriched for *Esrrb* binding and contained an *Esrrb* binding motif-like sequence (AAAGGTCA) (Fig. 3A and B), suggesting *Esrrb* as another candidate factor for the enhancer activity of “*Bmp4*-5’-1.4 kb”. To investigate this hypothesis, we performed a luciferase reporter assay in TS cells. Consistent with the previous study, we found that “*Bmp4*-5’-1.4 kb” fragment showed enhancer activity (Fig. 3C). This enhancer activity was abolished by deletion of the *Esrrb* binding site in “*Bmp4*-5’-1.4 kb”, underscoring the importance of *Esrrb* binding for enhancer activity. Unexpectedly, the -1516 to -949 fragment that included the *Esrrb* but not the *Cdx2* binding motif showed enhancer activity at the comparable level with the full-length enhancer. In addition, deletion of the *Cdx2* binding motif had no effect on enhancer activity. Thus, in contrast with previous report, our results suggest that the *Cdx2* binding site is dispensable for enhancer activity. The requirement of *Cdx2* binding might be context dependent, but it should be noted that ChIP-seq data sets of *Cdx2* in TS cells obtained by independent

groups did not detect *Cdx2* binding in this region (Chuong et al., 2013; Huang et al., 2017; Latos et al., 2015).

2.4. *Bmp4*-5’-1.4 kb enhancer regulates *Bmp4* expression in TS cells and *in vivo*

To investigate the function of the endogenous “*Bmp4*-5’-1.4 kb” enhancer, we deleted almost the entire enhancer region by CRISPR/Cas9 in TS cells (Fig. 4A–D). We obtained 5 independent TS cell lines carrying the deletion allele. However, we could not obtain homozygous mutant cell lines, with the 5 lines all heterozygous for the deletion allele. It is possible that homozygous mutant cells were eliminated during cell culture due to severe down-regulation of *Bmp4* expression, although necessity of *Bmp4* expression for TS cell survival has not been demonstrated so far to our knowledge. RT-qPCR analysis revealed that *Bmp4*, but not *Cdx2* or *Esrrb* gene transcription were significantly decreased even in the heterozygous enhancer knockout TS cells following 3 to 4 passages after

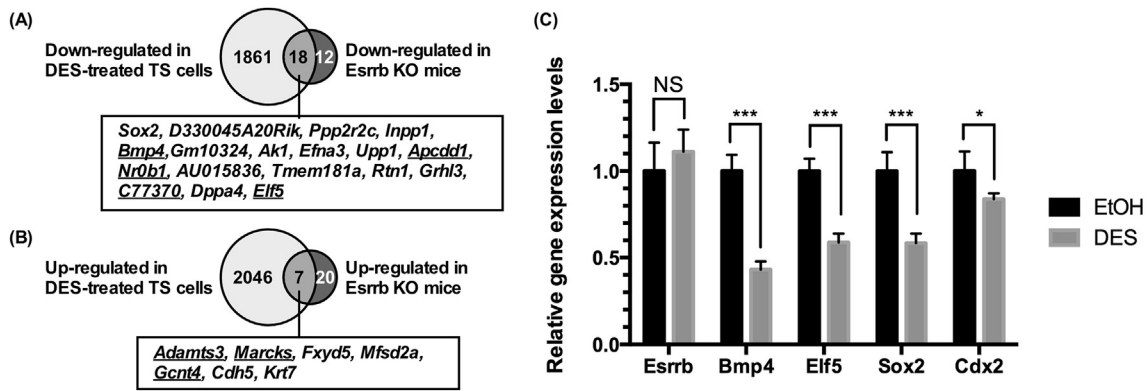


Fig. 2. Identification of potential downstream target genes of Esrrb using the TS cell system. (A) Comparison of genes down-regulated in DES-treated TS cells identified by RNA-seq analysis and down-regulated in ExE of homozygous *Esrrb* knockout embryo identified by microarray analysis (Fig. 1E). Genes that were identified as direct targets of Esrrb by BETA analysis are underlined. (B) Comparison of genes up-regulated in DES-treated TS cells identified by RNA-seq analysis and up-regulated in ExE of homozygous *Esrrb* knockout embryo identified by microarray analysis (Fig. 1E). Genes that were identified as direct targets of Esrrb by BETA analysis were underlined. (C) Validation of the RNA-seq results by RT-qPCR analysis. n = 3 for each sample. Results are shown with mean ± S.D. *p<0.1, ***p<0.01, NS: not significant, unpaired t-test.

single clonal isolation (Fig. 4E). These results further confirm that Esrrb binding to the “Bmp4-5’-1.4 kb” enhancer is required for the transcription of *Bmp4* in TS cells.

Next, to determine if the “Bmp4-5’-1.4 kb” enhancer regulates *Bmp4* expression *in vivo* as well, we established a knockout mouse line in which the enhancer was deleted by CRISPR/Cas9 (Fig. 4F). Heterozygous and homozygous knockout mice were born at expected Mendelian ratios

(wild-type: heterozygous knockout : homozygous knockout = 38 (31.4%) : 57 (47.1%) : 26 (21.5%)). To compare *Bmp4* transcript levels, we collected wild-type (n=4), heterozygous (n=4) and homozygous knockout (n=4) E6.5 embryos. RT-qPCR analysis revealed that *Bmp4* expression in homozygous knockout embryos was almost half compared to wild-type embryos (Fig. 4G). Thus the “Bmp4-5’-1.4 kb” enhancer, as in TS cells, functions *in vivo* to achieve correct levels of *Bmp4* expression.

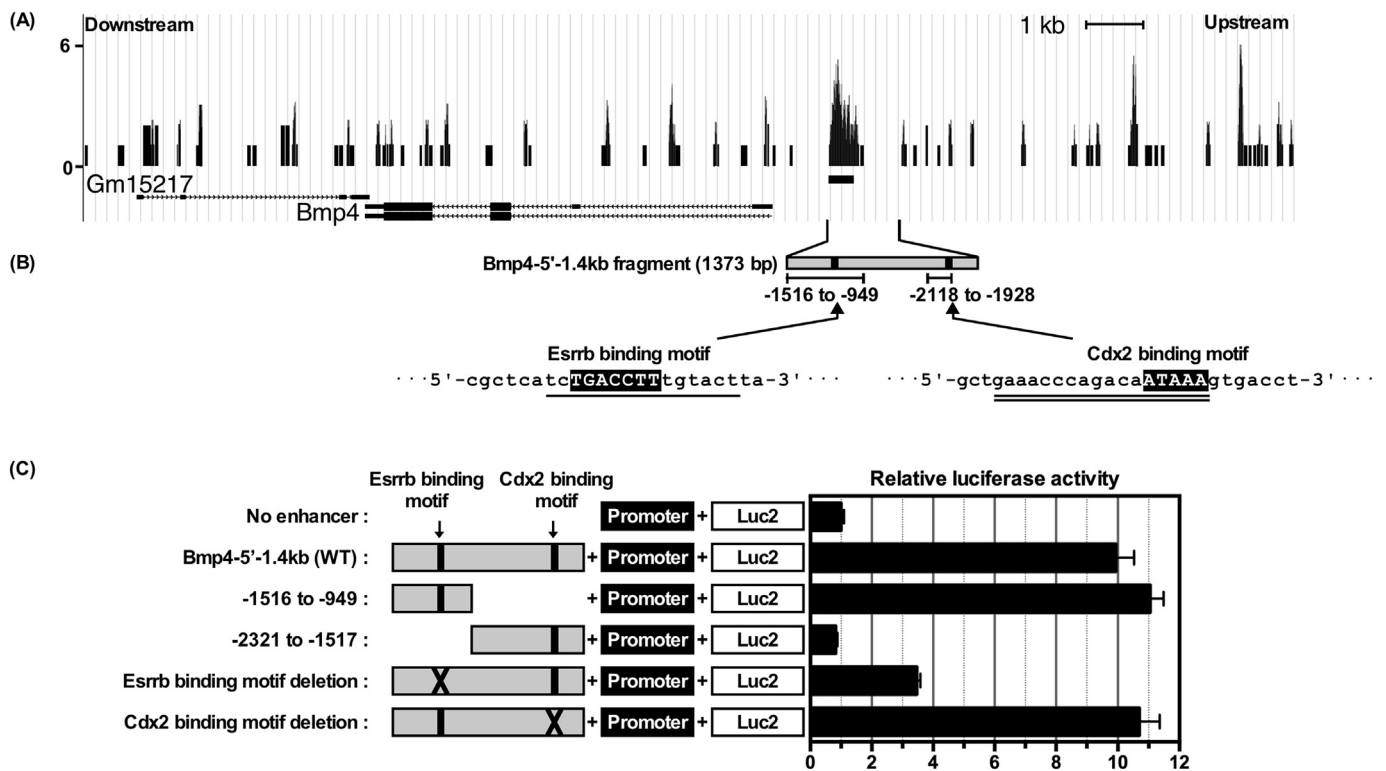


Fig. 3. Characterization of Esrrb-binding at the *Bmp4* enhancer in TS cells. (A) Peaks of Esrrb binding at the *Bmp4* locus visualized using the UCSC genome browser. (B) Location of the Bmp4-5’-1.4kb enhancer at the *Bmp4* locus. The positions of the Esrrb binding motif sequence in the –1516 to –949 region and the Cdx2 binding motif in the –2118 to –1928 region are indicated. Underlined nucleotide sequence around the Esrrb binding motif was deleted in the “Esrrb binding motif deletion” reporter construct illustrated in (C). Double underlined nucleotide sequence around the Cdx2 binding motif was deleted in the “Cdx2 binding motif deletion” reporter construct illustrated in (C). (C) Results of the luciferase reporter assay in TS cells. Schematic representations of reporter construct structures on the left. n = 4 for each sample.

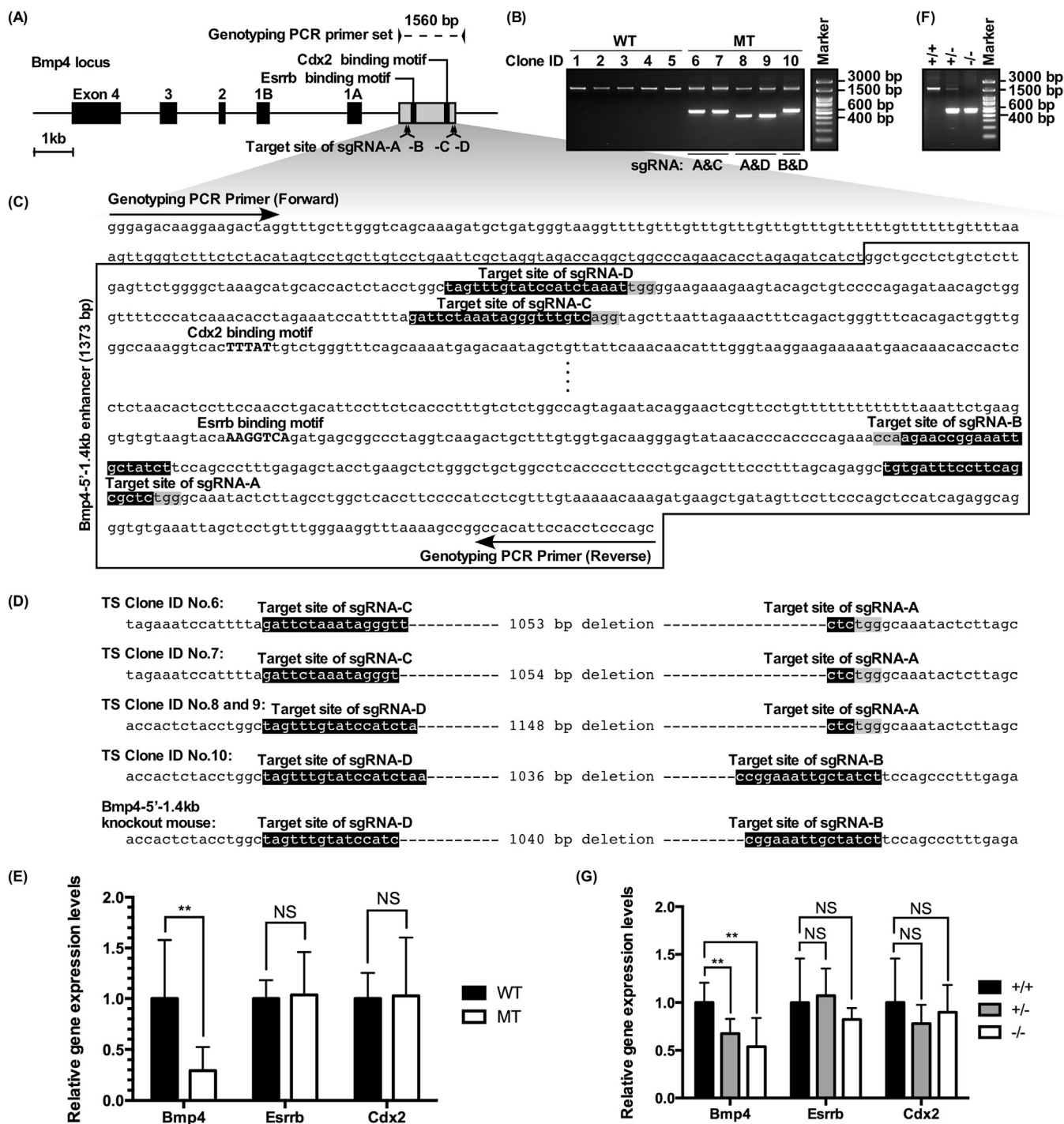


Fig. 4. Effect on endogenous *Bmp4* gene transcription by deletion of Esrrb-binding *Bmp4* enhancer in TS cells and E6.5 mouse embryos. (A) Schematic representation of the mouse *Bmp4* locus. Exons of *Bmp4* are indicated by black boxes, and the “Bmp4-5’-1.4 kb” enhancer is indicated by a gray box. Esrrb and Cdx2 binding motifs in the enhancer region are indicated by bold black lines. Arrowheads indicate the positions of primers used for genotyping PCR. The expected amplicon size from the wild-type allele is 1560 bp. Arrows indicate the positions of target sites of sgRNAs. (B) Results of genotyping PCR analysis of wild-type (WT) and mutant (MT) TS cells. (C) Wild-type DNA sequence flanked by genotyping PCR primer binding regions, obtained from GenBank (CT009556.7). Sequence of the “Bmp4-5’-1.4 kb” enhancer is enclosed in a box. sgRNA target sequences are highlighted in black, adjacent to NGG protospacer adjacent motif (PAM) highlighted in gray. Esrrb and Cdx2 binding motifs are indicated by bold capital letters. (D) Results of DNA sequencing analyses of deletion alleles in mutant TS cells and the knockout mouse. The length of the deleted region and flanking DNA sequences are shown. (E) Results of RT-qPCR analysis in wild-type (WT) and mutant (MT) TS cells. n = 5 for each sample. Results are shown with mean ± S.D. **p < 0.05, NS: not significant, unpaired *t*-test. (F) Results of genotyping PCR analysis of wild-type (+/+), heterozygous enhancer knockout (+/-) and homozygous enhancer knockout (-/-) mice. (G) Results of RT-qPCR analysis in wild-type (+/+), heterozygous enhancer knockout (+/-) and homozygous enhancer knockout (-/-) E6.5 embryos. Results are shown with mean ± S.D. n = 4 for each sample. **p < 0.05, NS: not significant, unpaired *t*-test.

2.5. *Esrrb*-mediated *Bmp4* expression is required for correct specification of primordial germ cells in the embryo *in vivo*

It has been reported that homozygous *Bmp4* knockout embryos do not have any PGCs and heterozygotes have fewer PGCs than normal, suggesting *Bmp4* affects the size of the PGC founding population in a dosage-dependent manner (Lawson et al., 1999). Because *Bmp4* expression levels in the homozygous *Esrrb* knockout embryos were significantly lower than wild-type and heterozygous embryos at E6.5, we hypothesized that *Esrrb* function in ExE is required for generating the correct number of PGCs. To test this hypothesis, we first compared PGC numbers between homozygous *Esrrb* knockout ($n = 7$) and control (wild-type and heterozygous knockout, $n = 15$) E7.75 embryos by whole-mount immunostaining analysis using anti-Tfap2c antibody. The specific staining of PGCs by this antibody was confirmed by Sox2, another PGC marker, antibody (Fig. 5A). We found that PGC numbers were significantly decreased in *Esrrb* homozygous knockout embryos compared to wild-type and heterozygous knockout controls (Fig. 5B). Next, we examined PGC numbers in the “*Bmp4*-5’-1.4 kb” enhancer knockout mouse line. Consistent with results from the *Esrrb* knockout mouse line, PGC numbers in heterozygous ($n = 32$) and homozygous *Bmp4*-5’-1.4 kb knockout ($n = 16$) embryos were significantly lower compared to wild-type controls ($n = 26$) (Fig. 5C and D). These data strongly suggest that regulation of *Bmp4* expression by *Esrrb* is required for the establishment of correct PGC numbers *in vivo*. After around E7.0 stage, however, *Bmp4* is expressed not only in the ExE but also in the newly formed extra-embryonic mesoderm (ExM), where PGCs are localized, and a tetraploid complementation experiment previously revealed that *Bmp4* in the ExM is required for localization and survival of PGCs (Fujiwara et al., 2001). Is there a possibility that the low PGC number observed in the *Esrrb* knockout and *Bmp4* enhancer knockout embryos is caused by a reduction of *Bmp4* in the ExM rather than the ExE? We suggest this to be

unlikely, due to previous observations. First, *Bmp4* in the ExM is required for proper PGC localization but not critical for PGC numbers at the pre-somite stage (Fujiwara et al., 2001). Second, *Esrrb* is specifically detected in the chorion, where PGCs are not localized, as shown by *in situ* hybridization and immunohistochemistry analysis (Luo et al., 1997; Mitsunaga et al., 2004; Pettersson et al., 1996). Taken together, we conclude that *Esrrb* function in the ExE is required for proper PGC specification. Of note, it has been previously reported that *Esrrb* starts to be expressed in PGCs in the developing gonad at E11.5, while in ExE-derivatives it becomes undetectable after E8.5. A tetraploid rescue experiment, in which *Esrrb* knockout embryos were complemented with wild-type trophoblast compartments, revealed that the number of germ cells was significantly reduced in rescued embryos between E13.5 to E15.5. This result suggested that *Esrrb* in PGCs is likely involved in cell proliferation (Mitsunaga et al., 2004). Thus, *Esrrb* is a critical factor for PGC development, which is likely to be involved in both PGC specification and proliferation at two distinct developmental stages.

2.6. “*Bmp4*-5’-1.4 kb” enhancer knockout male mice shows sub-fertile phenotype

To assess the consequences of “*Bmp4*-5’-1.4 kb” enhancer deletion on the fertility of adult mice, homozygous knockout males were mated with wild-type females. Females with a visible mating plug were sacrificed during late pregnancy (16–18 days following plug) and the number of fetuses was counted. We found that only 50% (15/30) of females plugged by homozygous knockout males were pregnant, whereas 93% (14/15) of females plugged by control wild-type males were pregnant (Fig. 6A, Supplemental Table S6). In contrast to the significant difference in pregnancy rate, the litter size of pregnant females was not significantly different (wt: 11.64 ± 3.59 vs homo KO: 10.73 ± 4.77 [mean \pm S.D.]). We also observed that the testes of homozygous mutants were significantly

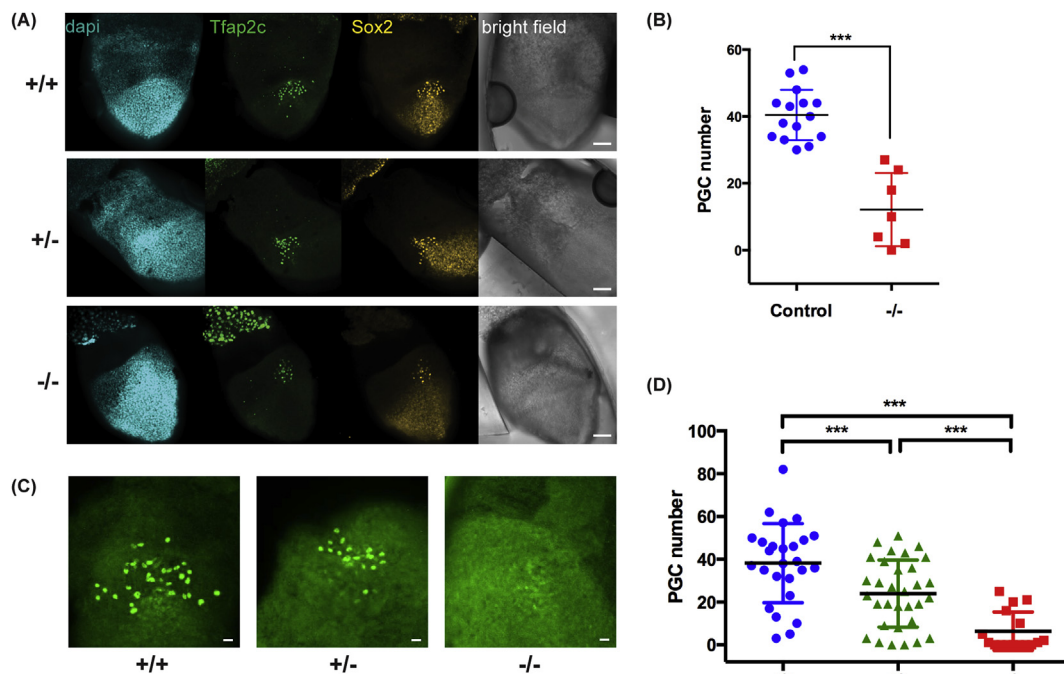


Fig. 5. Analysis of PGC numbers in *Esrrb* knockout and *Esrrb*-binding *Bmp4* enhancer knockout E7.75 mouse embryos. (A) Immunostaining of PGCs with anti-Tfap2c and anti-Sox2 antibodies in E7.75 embryos. 15 control (wild-type [+/+]) and heterozygous *Esrrb* knockout [+/-] and 7 homozygous *Esrrb* knockout [-/-] embryos were analyzed. Representative images are shown. All images were taken at the same magnification. Scale bar, 80 μ m. (B) Comparison of PGCs numbers between control and homozygous *Esrrb* knockout [-/-] E7.75 embryos, counted based on immunostaining analysis in (A). Results are shown with mean \pm SD. *** $p < 0.01$, unpaired *t*-test. (C) Immunostaining of PGCs in E7.75 embryos using anti-Tfap2c antibody. 26 wild-type (+/+), 32 heterozygous enhancer knockout (+/-) and homozygous enhancer knockout [-/-] embryos were analyzed. Representative images are shown. Scale bar, 20 μ m. (D) Comparison of PGC numbers between wild-type (+/+), heterozygous enhancer knockout (+/-) and homozygous enhancer knockout [-/-] E7.75 embryos, counted based on immunostaining analysis in (C). Results are shown with mean \pm SD. *** $p < 0.01$, Tukey-Kramer method.

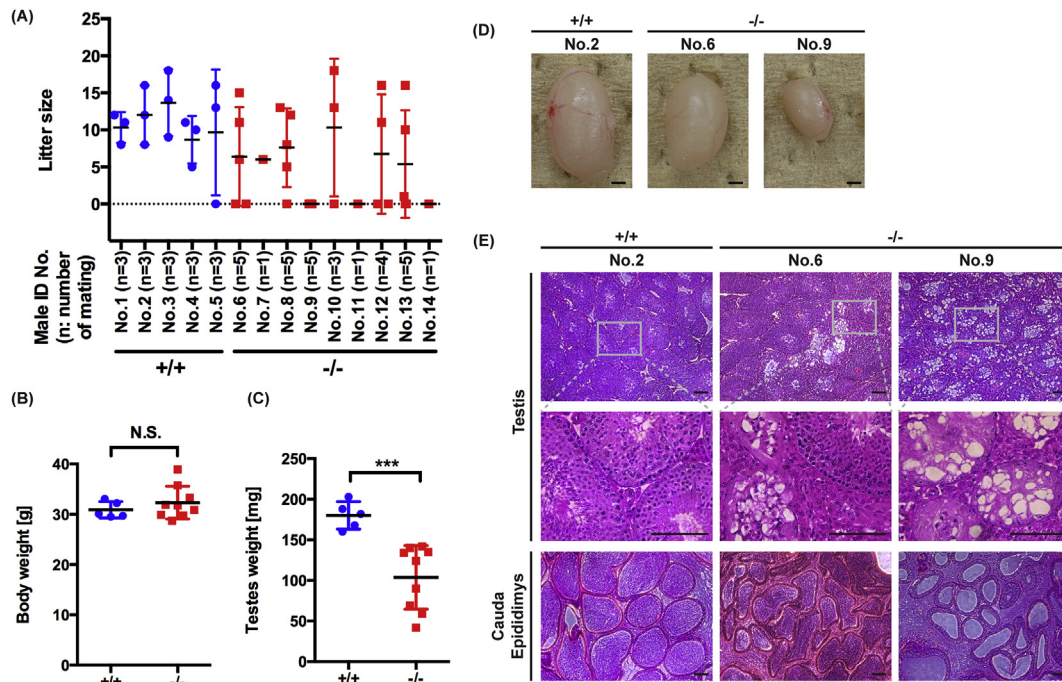


Fig. 6. Fertility of *Esrrb*-binding *Bmp4* enhancer knockout adult males. (A) Comparison of litter sizes of wild-type females mated with either wild-type (+/+) or homozygous enhancer knockout (-/-) males. 5 wild-type and 9 homozygous knockout males were used for mating, and the number of matings performed by each male are noted in brackets. (B, C) Comparison of body weight (B) and testis weight (C) between wild-type (+/+, n = 5) and homozygous enhancer knockout (-/-, n = 9) males used for mating tests in (A) at 6 months of age. Results are shown with mean \pm SD. *** $p < 0.01$, NS: not significant, unpaired *t*-test. (D) Morphology of testis of wild-type (+/+) and homozygous enhancer knockout males used for mating tests in (A). Scale bar, 1 mm. (E) H&E staining of testis and caudal epididymis of wild-type (+/+) and homozygous enhancer knockout males used for mating tests in (A). Scale bar, 200 μ m.

smaller compared to wild-type control males, whereas body weights were comparable (Fig. 6B–D). Examination of H&E-stained paraffin-embedded testes sections revealed that mutant mice have more seminiferous tubules lacking germ cells, including spermatogonia, than wild type mice (Fig. 6E). These results suggested that the decreased PGC numbers due to insufficient *Bmp4* expression in the ExE of the post-implantation embryo resulted in a sub fertile phenotype in adult males. Because *Bmp4* signaling is known to be required for spermatogenesis, it is possible that the sub fertile phenotype of the “*Bmp4*-5’-1.4 kb” enhancer knockout mice stemmed from a combination of reduced PGCs in the fetus and failure of spermatogenesis during later development. Requirement of the “*Bmp4*-5’-1.4 kb” enhancer for *Bmp4* transcription in cells related to spermatogenesis needs to be further explored. It is currently unclear why some homozygous knockout males can sometimes produce normal-sized litters, and sometimes cannot impregnate females. This phenotype can not be explained by the exhaustion of germ cells from the testis, because the same males could produce normal-sized litters at a later time (Supplemental Table S6). A likely explanation is that sperm concentration in the ejaculated semen was variable because of partial depletion of spermatogenic cells in seminiferous tubules.

In conclusion, taking advantage of the TS cell system and knockout mouse technology, we showed that *Esrrb* directly regulates *Bmp4* transcription in the ExE. This is a significant discovery because no upstream factor regulating *Bmp4* in ExE has been identified previously. However, our results also suggest that *Esrrb* alone might not be sufficient for enhancer activity of the “*Bmp4*-5’-1.4 kb” region, but requires other factors as well, because a mutant “*Bmp4*-5’-1.4 kb” fragment without *Esrrb* binding motif still showed weak enhancer activity (Fig. 3C). In addition, *Bmp4* expression was not completely lost even when the “*Bmp4*-5’-1.4 kb” enhancer region was homozygously deleted (Fig. 4G), further suggesting that there are other enhancers or co-factors at play. Therefore, additional investigation of the upstream regulators of *Bmp4* transcription is essential to elucidate the molecular mechanism behind PGC induction.

3. Materials and methods

3.1. Mice

Details of the *Esrrb* knockout mouse line used in this study are described elsewhere (Luo et al., 1997). CRISPR knockout mice were generated on the C57BL/6JMSlc (Japan SLC, Inc.) background. Wild-type Slc:ICR females (Japan SLC, Inc.) were used for mating tests. All animal work was carried out by following the Canadian Council on Animal Care Guidelines for Use of Animals in Research and Laboratory Animal Care under protocols approved by the Centre for Phenogenomics Animal Care Committee (protocol number: 20–0026H) or by following Fundamental Guidelines for Proper Conduct of Animal Experiments and Related Activities in Academic Research Institutions under the jurisdiction of the Ministry of Education, Culture, Sports, Science and Technology of Japan approved by the ethics committee for animal use and welfare in Tokushima University (T27-84).

3.2. Pre- and post-implantation embryo collection, immunostaining and imaging

E4.5 blastocysts were obtained by culturing fertilized eggs collected from the oviducts of ICR females. E4.75 blastocysts were obtained by flushing uteri from ICR females with M2 medium (Specialty Media, Chemicon). Fixation, permeabilization, immunostaining, and blocking were performed as previously described (Yamanaka et al., 2010). E5.5 post-implantation embryos were dissected from the uteri of pregnant females. Fixation was performed in 4% paraformaldehyde (PFA) for 15 min, permeabilization in 0.5% Triton-PBS for 20 min and blocking in 10% BSA, 5% serum in 0.1% Triton-PBS for 3 h at room temperature. E7.75 embryos were obtained from natural mated females or from females into which *in vitro* fertilized eggs have been transplanted. After the Reichert’s membranes were cleared and the ectoplacental cones were

trimmed away, the embryos were fixed in 4% PFA in PBS for 15 min, followed by storing in PBS-0.1% tween (PBT) at 4 °C overnight. After making a tiny cut into the exocoeloms, embryos were permeabilized in PBS-0.5% Triton for 20 min, blocked with PBT with 10% BSA and 5% Normal Donkey Serum or Fetal bovine serum for 8 h. Both pre- and post-implantation embryos were incubated with primary antibodies overnight at 4 °C, rinsed, and incubated with secondary antibodies for at least 1 h at room temperature. Primary antibodies used in this study include mouse anti-Esrrb 1:200 (Perseus Proteomics, PP-H6705-00), goat anti-Oct4 1:100 (Santa Cruz, sc-8628), rabbit anti-Cdx2 1:200 (James et al., 1994), rabbit anti-AP-2 γ 1:100 (Santa Cruz, sc-8977) and goat anti-Sox2 (R & D Systems, AF 2018, 1:100). Secondary antibodies include DyLight 549 conjugated donkey anti-mouse IgG (H + L), DyLight 488 conjugated donkey anti-rabbit IgG (H + L) (Jackson ImmunoResearch) and Alexa Fluor 488 conjugated donkey anti-rabbit IgG (H + L) (Jackson ImmunoResearch). Images were acquired using a Zeiss Axiovert 200 inverted microscope equipped with a Hamamatsu C9100-13 EM-CCD camera, a Quorum spinning disk confocal scan head and Volocity acquisition software (PerkinElmer). Z-stacks were taken at 1 μ m intervals with a 20x air objective (NA = 0.75). Images of *Bmp4* enhancer knockout embryos were acquired using a Nikon A1R confocal microscope with NIS Elements software (Nikon). Z-stacks were taken at 2 μ m intervals with a 20x dry objective (NA = 0.75). Images were analyzed with FIJI software (Schindelin et al., 2012). After imaging, the genotypes of the embryos were confirmed by genotyping PCR using REExtract-N-Amp kit (Sigma-Aldrich) according to the manufacturer's instructions.

3.3. Microarray analysis

Post-implantation embryos were dissected from the uteri of pregnant females at E6.5, and were split into two pieces at the border between ExE and embryo proper. The pieces of ExE and overlying VE from 20 to 25 embryos were pooled based on genotype, and three replicates for both wild-type and *Esrrb* homozygous knockout samples were prepared for microarray analysis. Genotyping was performed using the other pieces containing the embryo proper (see Luo et al., 1997 for genotyping protocol). Total RNA was extracted using Trizol (Thermo Fisher Scientific) according to the manufacturer's instructions, and the quality of the RNA was assessed by BioAnalyzer (Agilent Genomics) to confirm RIN values were > 9.6. 100 ng of RNA from each pooled sample was used to generate cDNA, which was then fragmented and labeled using the WT Expression Kit (Ambion) according to the manufacturer's instructions. cDNA was then hybridized to Mouse 1.0 ST gene array v1 (Affymetrix) according to the manufacturer's protocol, and scanned with an Affymetrix GeneChip Scanner 7G. The raw data was imported and normalized using the affy R package v.1.44.0 (Gautier et al., 2004), and analyzed using the limma R package v3.22.7 (Ritchie et al., 2015). Heat maps were generated in R from the normalized expression data, selecting only genes that were differentially expressed based on limma output (FDR corrected).

3.4. Trophoblast stem cell culture

TS cell line F4 derived from E3.5 blastocyst was used in this study (Rugg-Gunn et al., 2012). TS cells were maintained in RPMI1640 (Sigma-Aldrich) supplemented with 20% FBS (Life Technologies), 1 mM sodium pyruvate (Life Technologies), 50 U/ml penicillin, 50 μ g/ml streptomycin, 100 μ M 2-mercaptoethanol (Sigma-Aldrich), 2 mM Glutamax (Life Technologies), 25 ng/ml FGF4 (R & D Systems), and 1 μ g/ml heparin (Sigma-Aldrich), with 70% of the media preconditioned by mitotically inactivated E12.5 embryonic fibroblasts (70CM + F4H medium) (Tanaka et al., 1998). For DES treatment experiment, 3.2×10^5 , 1.6×10^5 , 8×10^4 or 1×10^4 TS cells were grown in 6-well plates for 1, 2, 3, 6 days, respectively, in 70CM + F4H medium in the presence of DES (20 μ M) or the vehicle (ethanol). For TS cell differentiation, 1×10^4 cells were grown for 6 days in 6-well plates in 70CM medium without FGF4 and heparin.

3.5. ChIP-sequencing

Preparation of the ChIP-seq library was performed according to the protocol described by Schmidt and colleagues (Schmidt et al., 2009). In brief, trophoblast stem cells were fixed with formaldehyde, lysed and then sonicated with a Misonix Sonicator 3000. The lysate is incubated with ~15 μ g anti-Esrrb antibody (Perseus Proteomics, PP-H6705-00) bound to Dynabeads (Invitrogen), washed, and the bound chromatin eluted. The eluate was reverse-crosslinked, and treated with proteinase K (Invitrogen) and RNase A (Ambion). The ChIP-enriched and corresponding input genomic DNA libraries were prepared using the Illumina Genomic Sample Preparation Kit (Illumina) according to the manufacturer's instruction, and sequenced on the HiSeq 2000 sequencer (Illumina) at the Centre for Applied Genomics (TCAG) facility at the Hospital for Sick Children.

FASTQ sequences were aligned to the mm9 genome using Bowtie2 v.2.2.3 (Langmead and Salzberg, 2012). Peak-calling was performed on the ChIP-seq library using MACS v.2.2.1 (Zhang et al., 2008) using the corresponding input DNA library as control. ChIP-seq peaks were analyzed using GREAT software v3.0.0 (McLean et al., 2010) to identify potentially regulated targets, and later combined with RNA-seq data for analysis by Binding and Expression Target Analysis (BETA) v1.0.7 (Wang et al., 2013). Enriched motifs in the ChIP-seq peaks were identified and annotated using MEME suite (v4.9.1) (Bailey et al., 2009), the JASPAR 2010 core database (Portales-Casamar et al., 2010) and transcription factor binding motifs identified by Chen and colleagues (Chen et al., 2008).

3.6. RNA-sequencing

Total RNA was extracted from TS cells treated with DES or vehicle (ethanol) for 2 days using TRIZOL reagent with PureLink RNA Micro Kit (Thermo Fisher Scientific). Single-end 100bp RNA-sequencing libraries were prepared using TruSeq Stranded Sample Prep Kit with human/mouse/rat Ribo Zero Gold, and sequenced with HiSeq 2500 at The Centre for Applied Genomics (TCAG) facility at the Hospital for Sick Children.

FASTQ sequences were aligned to the mm9 genome using STAR v2.3.1z12 (Dobin et al., 2013) and quantified using HTSeq v0.6.1 (Anders et al., 2015). Differential expression analysis was performed using DESeq v.1.18.0 (Anders and Huber, 2010). For validation of the results, cDNAs were synthesized from the same RNA used for RNA-sequencing with QuantiTect Reverse Transcription Kit (Qiagen). RT-qPCR was performed with the LightCycler 480 system (Roche) using LightCycler 480 SYBR Green I Master (Roche). Primer sequences used for real-time qPCR are listed in Supplemental Table S5.

3.7. Luciferase reporter assay

All test fragments were inserted into pGL4.10[luc2] vector (Promega) containing *Hspa1a* promoter. "Esrrb binding motif deletion" and "Cdx2 binding motif deletion" fragments were generated using Phusion Site-Directed Mutagenesis Kit (Thermo Fisher Scientific). Primer sequences used to amplify these DNA fragments are listed in Supplemental Table S5. DNA transfection into TS cells was essentially carried out as described elsewhere with minor modifications (Hayakawa et al., 2015). Briefly, 1.5×10^4 TS cells were seeded in 360 μ l of 70CM + F4H medium to wells of 24-well plate the day before transfection. 1 μ g of test constructs and 5 ng of pGL4.74 (Promega) were mixed and made up to 40 μ l with jetPRIME buffer, and then mixed with 1.8 μ l of jetPRIME reagent, followed by incubation for 10 min at room temperature. The jetPRIME-DNA mixture was dropped into culture plate containing TS cells and incubated for 4 h at 37 °C in 5% CO₂/95% air, and then medium was replaced with fresh 70CM + F4H medium and incubated another 20 h. Luciferase activity was determined using Dual-Luciferase Reporter Assay System (Promega) and Lumat LB9507 (Berthold) according to manufacturer's instructions. Assays were performed in quadruplicate, and average values with S.D. were calculated.

3.8. Genome editing by CRISPR/Cas9 system in TS cells

To prepare the plasmids expressing hCas9 and sgRNA, two pairs of sense and antisense oligos were annealed and inserted into *BbsI* site of px459 (addgene #48139) (Ran et al., 2013). These sgRNAs, sgRNA-A, -B, -C and -D, were designed to flank the *Bmp4*-5′-1.4 kb enhancer to delete the region that contains the *Esrrb* binding motif (Fig. 4A). Plasmid DNA transfection into TS cells was performed by method described elsewhere with minor modifications (Hayakawa et al., 2015). Briefly, 7.5×10^4 TS cells were seeded in 2 ml of 70CM + F4H medium to a well of 6-well plate and incubated for 24 h at 37°C in 5% CO₂/95% air. 2.5 µg each of two plasmids, containing either sgRNA-A or C /-A or -D /-B or -D, were mixed and made up to 200 µl with jet PRIME buffer, and then mixed with 9 µl of jetPRIME reagent, followed by incubation for 10 min at room temperature. The jetPRIME-DNA mixture was dropped into culture plate containing TS cells and incubated for 4 h at 37°C in 5% CO₂/95% air, and then medium was replaced with fresh 70CM + F4H medium and incubated another 20 h. The TS cells were subjected to selection with 4 µg/ml of Puromycin for additional 48 h followed by the culture without puromycin for 9 days until colonies formed. After sub-culture once, single cell cloning was performed by serial dilution in 96-well plate, and 5 independent clones were obtained. As a control, 5 wild-type TS cell clones were also obtained by serial dilution of TS cells without transfection. Genotyping PCR was performed with a primer set designed to amplify entire *Bmp4*-5′-1.4 kb enhancer region. The sequences of oligos are listed in Supplemental Table S5.

3.9. Generation of *Bmp4* enhancer knockout mouse line by CRISPR/Cas9 system

hCas9 mRNA and sgRNA were synthesized by a method described in elsewhere (Hashimoto and Takemoto, 2015) with minor modifications. Briefly, to synthesize hCas9 mRNA, pSP64 plasmid harboring the coding sequence of hCas9 was linearized by digestion with *SalI* and used as template for *in vitro* transcription using mMESSAGE mMACHINE SP6 Transcription kit (Thermo Fisher Scientific). To synthesize sgRNAs, two pairs of sense and antisense oligos were annealed and inserted into the *BsaI* site of the DR274 (addgene, #42250) (Hwang et al., 2013). The target sites of these sgRNAs (-B and -D) are same as those used in TS cells described above (Fig. 4A), and the sequences of oligos are listed in Supplemental Table S5. The plasmids were digested with *DraI*, and sgRNAs were synthesized using MEGAscript T7 Transcription Kit (Thermo Fisher Scientific). The synthesized mRNA and sgRNAs were purified using MEGAclear Transcription Clean-Up Kit and dissolved with Opti-MEM I (Thermo Fisher Scientific) after ethanol precipitation. Fertilized eggs were obtained by *in vitro* fertilization by method described elsewhere (Takeo and Nakagata, 2015) with minor modifications. Briefly, oocytes were collected from oviducts of 4-weeks old C57BL/6JJmsSlc (Japan SLC) females superovulated by intraperitoneal administration of CARD HyperOva (Kyudo) followed by human chorionic gonadotropin (hCG). Sperms were collected from a caudal epididymis of 3-month-old C57BL/6JJmsSlc male, and then preincubated in Fertiup Mouse Sperm Preincubation Media (Kyudo). Insemination was done in HTF media (ark resource) and incubated at 37 °C in atmosphere containing 5% CO₂ for 3 h. Fertilized eggs were washed to remove cumulus cells and sperms, and incubated in mWM medium (ark resource) for 1hr. Electroporation of fertilized eggs was performed in Opti-MEM I media containing Cas9 mRNA (400 ng/µl) and gRNAs (100 ng/µl, each) using Genome Editor (BEX) as described in elsewhere (Hashimoto and Takemoto, 2015). In this study, the electroporation condition was 25 V (3 msec ON + 97 msec OFF) x 5 times. The eggs were incubated another 24 h in mWM media and 2-cell-embryos were transplanted into oviduct of pseudopregnant recipient mice. Genotyping PCR was performed with a primer set designed to amplify entire *Bmp4*-5′-1.4 kb enhancer region. The sequences of oligos are listed in Supplemental Table S5.

3.10. Fertility testing and histology

2- to 5-month-old wild-type and homozygous *Bmp4*-enhancer knockout males were housed in individual cages. 2- to 4-month-old wild-type females (Slc:ICR) were placed into each cage and checked for a vaginal plug daily. Plugged females were removed and dissected at 16- to 18 days post coitum to count offspring number. Males used for fertility testing were dissected at 6-month old. Testes and caudal epididymides were fixed in Bouin's fixative at 4 °C 12 h, processed for paraffin embedding using an automatic tissue processor (Tissue-Tek VIP-5-Jr), and sectioned at thickness of 3 µm. The sections were stained with hematoxylin and eosin using an autostainer (Tissue-Tek, DRS 2000). Images were taken with an inverted phase contrast microscope (Leica, DMIL LED) equipped with a camera (Leica, DFC295).

3.11. Resources

Information on key resources is provided in the KRT table.

3.12. Key resources table

Reagent or resource	Source	Identifier
Antibodies		
Mouse monoclonal anti- <i>Esrrb</i>	Cosmo Bio Co (Perseus Proteomics)	Cat# PPH670500; RRID:AB_567457
Goat polyclonal anti-Oct-3/4 (N-19)	Santa Cruz Biotechnology	Cat# sc-8628; RRID:AB_653551
Rabbit polyclonal anti-Cdx2	James et al. (1994)	N/A
Rabbit polyclonal anti-AP-2γ	Santa Cruz Biotechnology	Cat# sc-8977; RRID:AB_2286995
Goat polyclonal anti-Sox2	R and D Systems	Cat# AF 2018; RRID:AB_355110
Bacterial and Virus Strains		
N/A		
Biological Samples		
N/A		
Chemicals, Peptides, and Recombinant Proteins		
Diethylstilbestrol (DES)	Sigma-Aldrich	Cat# D4628-5G
Critical Commercial Assays		
Dual-Luciferase Reporter Assay System	Promega	Cat# E1960
Deposited Data		
The microarray, RNA-seq and ChIP-seq datasets	This paper	GEO: GSE123363
Experimental Models: Cell Lines		
Trophoblast stem cell line F4	Rugg-Gunn et al. (2012)	N/A
Experimental Models: Organisms/Strains		
<i>Esrrb</i> knockout mice	Luo et al. (1997)	N/A
" <i>Bmp4</i> -5′-1.4kb" enhance knock out mice	This paper	N/A
Oligonucleotides		
See Supplemental Table S5		
Recombinant DNA		
Plasmid: px459	Ran et al. (2013)	addgene #48139
Plasmid: DR274	Hwang et al. (2013)	addgene, #42250
Software and Algorithms		
affy R package v.1.44.0	Gautier et al. (2004)	https://bioconductor.org/packages/release/bioc/html/affy.html
limma R package v3.22.7	Ritchie et al. (2015)	https://bioconductor.org/packages/release/bioc/html/limma.html
Bowtie2 v.2.2.3	Langmead and Salzberg (2012)	http://bowtie-bio.sourceforge.net/bowtie2/index.shtml
MACS v.2.2.1	Zhang et al. (2008)	N/A
GREAT software v3.0.0	McLean et al. (2010)	http://great.stanford.edu/public/html/
Binding and Expression Target Analysis (BETA) v1.0.7	Wang et al. (2013)	http://cistrome.org/BETA/

(continued on next page)

(continued)

Reagent or resource	Source	Identifier
MEME suite (v4.9.1)	Bailey et al. (2009)	http://meme-suite.org/
STAR v2.3.1z12	Dobin et al. (2013)	N/A
HTSeq v0.6.1	Anders et al. (2015)	https://htseq.readthedocs.io/en/release_0.11.1/
DESeq v.1.18.0	Anders and Huber (2010)	https://bioconductor.riken.jp/packages/3.0/bioc/html/DESeq.html
Other		
N/A		

Acknowledgements

This work was supported by JSPS KAKENHI Grant Number 15H06447 (E.O.). E.O. was supported by a postdoctoral fellowship from the Uehara Memorial Foundation and Study Abroad Grant Program from BioLegend/Tomy Digital Biology. O.H.T. was supported by a fellowship of the Human Frontier Science Program. We thank the Transgenic Core lab headed by Marina Gertsenstein at The Centre for Phenogenomics (TCP), Toronto for transgenic services, The Centre for Applied Genomics (TCAG) facility at the Hospital for Sick Children and Support Centre for Advanced Medical Sciences of Tokushima University Graduate School of Biomedical Sciences for technical support. We thank all members of the Department of Genetic Engineering and Animal Research Resources, Tokushima University for help and valuable discussions.

Appendix A. Supplementary data

Supplementary data to this article can be found online at <https://doi.org/10.1016/j.ydbio.2019.07.008>.

Conflicts of interest

The authors declare no competing or financial interests.

Data availability

The microarray, RNA-seq and ChIP-seq datasets are deposited in GEO under accession number GSE123363.

Author contributions

Conceptualization: E.O., O.H.T., E.P., J.R.; Methodology: E.O., O.H.T., E.P.; Software: O.H.T.; Validation: E.O., L.L., K.C., C.Q.E.L., J.G.; Formal analysis: E.O., O.H.T., E.P., C.Q.E.L.; Investigation: E.O., O.H.T., E.P., L.L., K.C., C.Q.E.L., J.G.; Resources: E.O., O.H.T., E.P., L.L., K.C., C.Q.E.L., J.G.; Data curation: E.O., O.H.T.; Writing - original draft: E.O., O.H.T., E.P., L.L., K.C., C.Q.E.L., J.R.; Writing - review & editing: E.O., O.H.T., E.P., L.L., K.C., C.Q.E.L., J.R.; Visualization: E.O., O.H.T., E.P.; Supervision: J.R.; Project administration: E.O., J.R.; Funding acquisition: E.O., J.R.

References

Adachi, K., Nikaido, I., Ohta, H., Ohtsuka, S., Ura, H., Kadota, M., Wakayama, T., Ueda, H.R., Niwa, H., 2013. Context-dependent wiring of Sox2 regulatory networks for self-renewal of embryonic and trophoblast stem cells. *Mol. Cell* 52, 380–392.

Anders, S., Huber, W., 2010. Differential expression analysis for sequence count data. *Genome Biol.* 11, R106.

Anders, S., Pyl, P.T., Huber, W., 2015. HTSeq—a Python framework to work with high-throughput sequencing data. *Bioinformatics* 31, 166–169.

Bailey, T.L., Boden, M., Buske, F.A., Frith, M., Grant, C.E., Clementi, L., Ren, J., Li, W.W., Noble, W.S., 2009. MEME SUITE: tools for motif discovery and searching. *Nucleic Acids Res.* 37, W202–W208.

Chang, H., Matzuk, M.M., 2001. Smad5 is required for mouse primordial germ cell development. *Mech. Dev.* 104, 61–67.

Chen, X., Xu, H., Yuan, P., Fang, F., Huss, M., Vega, V.B., Wong, E., Orlov, Y.L., Zhang, W., Jiang, J., Loh, Y.H., Yeo, H.C., Yeo, Z.X., Narang, V., Govindarajan, K.R., Leong, B., Shahab, A., Ruan, Y., Bourque, G., Sung, W.K., Clarke, N.D., Wei, C.L., Ng, H.H.,

2008. Integration of external signaling pathways with the core transcriptional network in embryonic stem cells. *Cell* 133, 1106–1117.

Chu, G.C., Dunn, N.R., Anderson, D.C., Oxburgh, L., Robertson, E.J., 2004. Differential requirements for Smad4 in TGFbeta-dependent patterning of the early mouse embryo. *Development* 131, 3501–3512.

Chuong, E.B., Rumi, M.A., Soares, M.J., Baker, J.C., 2013. Endogenous retroviruses function as species-specific enhancer elements in the placenta. *Nat. Genet.* 45, 325–329.

de Sousa Lopes, S.M., Hayashi, K., Surani, M.A., 2007. Proximal visceral endoderm and extraembryonic ectoderm regulate the formation of primordial germ cell precursors. *BMC Dev. Biol.* 7, 140.

de Sousa Lopes, S.M., Roelen, B.A., Monteiro, R.M., Emmens, R., Lin, H.Y., Li, E., Lawson, K.A., Mummery, C.L., 2004. BMP signaling mediated by ALK2 in the visceral endoderm is necessary for the generation of primordial germ cells in the mouse embryo. *Genes Dev.* 18, 1838–1849.

Dobin, A., Davis, C.A., Schlesinger, F., Drenkow, J., Zaleski, C., Jha, S., Batut, P., Chaisson, M., Gingeras, T.R., 2013. STAR: ultrafast universal RNA-seq aligner. *Bioinformatics* 29, 15–21.

Donnison, M., Beaton, A., Davey, H.W., Broadhurst, R., L'Huillier, P., Pfeffer, P.L., 2005. Loss of the extraembryonic ectoderm in Elf5 mutants leads to defects in embryonic patterning. *Development* 132, 2299–2308.

Extavour, C.G., Akam, M., 2003. Mechanisms of germ cell specification across the metazoans: epigenesis and preformation. *Development* 130, 5869–5884.

Festuccia, N., Owens, N., Navarro, P., 2018. Esrrb, an estrogen-related receptor involved in early development, pluripotency, and reprogramming. *FEBS Lett.* 592, 852–877.

Fujiwara, T., Dunn, N.R., Hogan, B.L., 2001. Bone morphogenetic protein 4 in the extraembryonic mesoderm is required for allantois development and the localization and survival of primordial germ cells in the mouse. *Proc. Natl. Acad. Sci. U. S. A.* 98, 13739–13744.

Gautier, L., Cope, L., Bolstad, B.M., Irizarry, R.A., 2004. affy—analysis of Affymetrix GeneChip data at the probe level. *Bioinformatics* 20, 307–315.

Goolam, M., Scialdone, A., Graham, S.J.L., Macaulay, I.C., Jedrusik, A., Hupalowska, A., Voet, T., Marioni, J.C., Zemicka-Goetz, M., 2016. Heterogeneity in Oct4 and Sox2 targets biases cell fate in 4-cell mouse embryos. *Cell* 165, 61–74.

Guo, G., Huss, M., Tong, G.Q., Wang, C., Li, Sun, L., Clarke, N.D., Robson, P., 2010. Resolution of cell fate decisions revealed by single-cell gene expression analysis from zygote to blastocyst. *Dev. Cell* 18, 675–685.

Hashimoto, M., Takemoto, T., 2015. Electroporation enables the efficient mRNA delivery into the mouse zygotes and facilitates CRISPR/Cas9-based genome editing. *Sci. Rep.* 5, 11315.

Hayakawa, K., Himeno, E., Tanaka, S., Kunath, T., 2015. Isolation and manipulation of mouse trophoblast stem cells. *Curr. Protoc. Stem Cell Biol.* 32, 1E.4.1–1E.4.32.

Hayashi, K., Kobayashi, T., Umino, T., Goitsuka, R., Matsui, Y., Kitamura, D., 2002. SMAD1 signaling is critical for initial commitment of germ cell lineage from mouse epiblast. *Mech. Dev.* 118, 99–109.

Huang, D., Guo, G., Yuan, P., Ralston, A., Sun, L., Huss, M., Mistri, T., Pinello, L., Ng, H.H., Yuan, G., Ji, J., Rossant, J., Robson, P., Han, X., 2017. The role of Cdx2 as a lineage specific transcriptional repressor for pluripotent network during the first developmental cell lineage segregation. *Sci. Rep.* 7, 17156.

Hwang, W.Y., Fu, Y., Reyon, D., Maeder, M.L., Tsai, S.Q., Sander, J.D., Peterson, R.T., Yeh, J.R., Joung, J.K., 2013. Efficient genome editing in zebrafish using a CRISPR-Cas system. *Nat. Biotechnol.* 31, 227–229.

James, R., Erler, T., Kazenwadel, J., 1994. Structure of the murine homeobox gene cdx-2. Expression in embryonic and adult intestinal epithelium. *J. Biol. Chem.* 269, 15229–15237.

Kidder, B.L., Palmer, S., 2010. Examination of transcriptional networks reveals an important role for TCFAP2C, SMARCA4, and EOMES in trophoblast stem cell maintenance. *Genome Res.* 20, 458–472.

Langmead, B., Salzberg, S.L., 2012. Fast gapped-read alignment with Bowtie 2. *Nat. Methods* 9, 357–359.

Latos, P.A., Goncalves, A., Oxley, D., Mohammed, H., Turro, E., Hemberger, M., 2015. Fgf and Esrrb integrate epigenetic and transcriptional networks that regulate self-renewal of trophoblast stem cells. *Nat. Commun.* 6, 7776.

Lawson, K.A., Dunn, N.R., Roelen, B.A., Zeinstra, L.M., Davis, A.M., Wright, C.V., Korving, J.P., Hogan, B.L., 1999. Bmp4 is required for the generation of primordial germ cells in the mouse embryo. *Genes Dev.* 13, 424–436.

Luo, J., Sladek, R., Bader, J.A., Matthyssen, A., Rossant, J., Giguère, V., 1997. Placental abnormalities in mouse embryos lacking the orphan nuclear receptor ERR-beta. *Nature* 388, 778–782.

McLean, C.Y., Bristor, D., Hiller, M., Clarke, S.L., Schaar, B.T., Lowe, C.B., Wenger, A.M., Bejerano, G., 2010. GREAT improves functional interpretation of cis-regulatory regions. *Nat. Biotechnol.* 28, 495–501.

Mitsunaga, K., Araki, K., Mizusaki, H., Morohashi, K., Haruna, K., Nakagata, N., Giguère, V., Yamamura, K., Abe, K., 2004. Loss of PGC-specific expression of the orphan nuclear receptor ERR-beta results in reduction of germ cell number in mouse embryos. *Mech. Dev.* 121, 237–246.

Murohashi, M., Nakamura, T., Tanaka, S., Ichise, T., Yoshida, N., Yamamoto, T., Shibuya, M., Schlessinger, J., Gotoh, N., 2010. An FGF4-FRS2alpha-Cdx2 axis in trophoblast stem cells induces Bmp4 to regulate proper growth of early mouse embryos. *Stem Cells* 28, 113–121.

Pesce, M., Klingner, F.G., De Felici, M., 2002. Derivation in culture of primordial germ cells from cells of the mouse epiblast: phenotypic induction and growth control by Bmp4 signalling. *Mech. Dev.* 112, 15–24.

Pettersson, K., Svensson, K., Mattsson, R., Carlsson, B., Ohlsson, R., Berkenstam, A., 1996. Expression of a novel member of estrogen response element-binding nuclear

- receptors is restricted to the early stages of chorion formation during mouse embryogenesis. *Mech. Dev.* 54, 211–223.
- Portales-Casamar, E., Thongjuea, S., Kwon, A.T., Arenillas, D., Zhao, X., Valen, E., Yusuf, D., Lenhard, B., Wasserman, W.W., Sandelin, A., 2010. JASPAR 2010: the greatly expanded open-access database of transcription factor binding profiles. *Nucleic Acids Res.* 38, D105–D110.
- Ran, F.A., Hsu, P.D., Wright, J., Agarwala, V., Scott, D.A., Zhang, F., 2013. Genome engineering using the CRISPR-Cas9 system. *Nat. Protoc.* 8, 2281–2308.
- Ritchie, M.E., Phipson, B., Wu, D., Hu, Y., Law, C.W., Shi, W., Smyth, G.K., 2015. Limma powers differential expression analyses for RNA-sequencing and microarray studies. *Nucleic Acids Res.* 43, e47.
- Rugg-Gunn, P.J., Cox, B.J., Lanner, F., Sharma, P., Ignatchenko, V., McDonald, A.C., Garner, J., Gramolini, A.O., Rossant, J., Kislinger, T., 2012. Cell-surface proteomics identifies lineage-specific markers of embryo-derived stem cells. *Dev. Cell* 22, 887–901.
- Schindelin, J., Arganda-Carreras, I., Frise, E., Kaynig, V., Longair, M., Pietzsch, T., Preibisch, S., Rueden, C., Saalfeld, S., Schmid, B., Tinevez, J.Y., White, D.J., Hartenstein, V., Eliceiri, K., Tomancak, P., Cardona, A., 2012. Fiji: an open-source platform for biological-image analysis. *Nat. Methods* 9, 676–682.
- Schmidt, D., Wilson, M.D., Spyrou, C., Brown, G.D., Hadfield, J., Odom, D.T., 2009. ChIP-seq: using high-throughput sequencing to discover protein-DNA interactions. *Methods* 48, 240–248.
- Strumpf, D., Mao, C.A., Yamanaka, Y., Ralston, A., Chawengsaksophak, K., Beck, F., Rossant, J., 2005. *Cdx2* is required for correct cell fate specification and differentiation of trophoblast in the mouse blastocyst. *Development* 132, 2093–2102.
- Takeo, T., Nakagata, N., 2015. Superovulation using the combined administration of inhibin antiserum and equine chorionic gonadotropin increases the number of ovulated oocytes in C57BL/6 female mice. *PLoS One* 10, e0128330.
- Tanaka, S., Kunath, T., Hadjantonakis, A.K., Nagy, A., Rossant, J., 1998. Promotion of trophoblast stem cell proliferation by FGF4. *Science* 282, 2072–2075.
- Tremblay, G.B., Kunath, T., Bergeron, D., Lapointe, L., Champigny, C., Bader, J.A., Rossant, J., Giguère, V., 2001a. Diethylstilbestrol regulates trophoblast stem cell differentiation as a ligand of orphan nuclear receptor ERR beta. *Genes Dev.* 15, 833–838.
- Tremblay, K.D., Dunn, N.R., Robertson, E.J., 2001b. Mouse embryos lacking *Smad1* signals display defects in extra-embryonic tissues and germ cell formation. *Development* 128, 3609–3621.
- Wang, S., Sun, H., Ma, J., Zang, C., Wang, C., Wang, J., Tang, Q., Meyer, C.A., Zhang, Y., Liu, X.S., 2013. Target analysis by integration of transcriptome and ChIP-seq data with BETA. *Nat. Protoc.* 8, 2502–2515.
- Yamanaka, Y., Lanner, F., Rossant, J., 2010. FGF signal-dependent segregation of primitive endoderm and epiblast in the mouse blastocyst. *Development* 137, 715–724.
- Ying, Y., Liu, X.M., Marble, A., Lawson, K.A., Zhao, G.Q., 2000. Requirement of *Bmp8b* for the generation of primordial germ cells in the mouse. *Mol. Endocrinol.* 14, 1053–1063.
- Ying, Y., Qi, X., Zhao, G.Q., 2001. Induction of primordial germ cells from murine epiblasts by synergistic action of BMP4 and BMP8B signaling pathways. *Proc. Natl. Acad. Sci. U. S. A.* 98, 7858–7862.
- Ying, Y., Zhao, G.Q., 2001. Cooperation of endoderm-derived BMP2 and extraembryonic ectoderm-derived BMP4 in primordial germ cell generation in the mouse. *Dev. Biol.* 232, 484–492.
- Yoshimizu, T., Obinata, M., Matsui, Y., 2001. Stage-specific tissue and cell interactions play key roles in mouse germ cell specification. *Development* 128, 481–490.
- Zhang, Y., Liu, T., Meyer, C.A., Eeckhoute, J., Johnson, D.S., Bernstein, B.E., Nusbaum, C., Myers, R.M., Brown, M., Li, W., Liu, X.S., 2008. Model-based analysis of chip-seq (MACS). *Genome Biol.* 9, R137.